4

Tectonophysics, 31 (1976) T21—T28

Letter Section

Rheological evidence for changes in the deformation mechanism of Solenhofen limestone towards low stresses

S.M. SCHMID

Research School of Earth Sciences, Australian National University, Canberra, A.C.T. (Australia)

(Submitted September 22, 1975; revised version accepted December 12, 1975)

ABSTRACT

Schmid, S.M., 1976. Rheological evidence for changes in the deformation mechanism of Solenhofen limestone towards low stresses. Tectonophysics, 31: T21—T28.

New rheological data on Solenhofen limestone at temperatures of 600—900°C show a transition into power-law creep with n-values around 4.5 followed by a second transition into low n-values ($n \sim 2$). It is suggested that the mechanism associated with low n-values is probably the active one in many geological situations involving flow in fine-grained carbonates and corresponds to superplastic phenomena known to occur in fine-grained metals.

INTRODUCTION

Constitutive equations for creep, relating strain rate and flow stress as observed in the laboratory, can only be extrapolated over many orders of magnitude in strain rate into geological environments provided no change in deformation mechanism (and consequently the form of the constitutive equations) takes place towards lower strain rates and stresses. Such changes, however, are well documented in the case of metals and attempts have been made to consider them in the treatment of tectonophysical problems. Fields of different flow regimes in rocks can be represented in a stress—temperature space in the form of "deformation maps", so far based mainly on theoretical considerations (Stocker and Ashby, 1973; Paterson, 1975 and Rutter, 1975).

Following suggestions by Paterson (1975) an attempt was made to produce geologically relevant deformation mechanisms at low stresses using high temperatures, given the limited range of laboratory strain rates. Some deformation mechanisms at low stresses are expected to be grain-size dependent (Coble- and Nabarro-Herring creep, superplastic phenomena). This is because in fine-grained materials, processes such as mass transfer by diffusion and/or grain-boundary sliding become more readily (i.e. at higher stresses) competitive with processes involving dislocation motion alone. Therefore, Solenhofen limestone was regarded as suitable material to explore such low-stress regimes (grain-size: 1—10 μm). Much is known already on the rheology of Solenhofen limestone at moderate temperatures up to 500°C (Rutter, 1974) and of coarser-grained Yule marble up to 800°C (Heard, 1963; Heard and Raleigh, 1972) but extrapolations into geological conditions based on these flow laws alone fail, at least in some geological environments (Schmid, 1975), in that they give unrealistically high estimates of flow stress. This suggests that other deformation mechanisms, for which the flow stress is more sensitive to strain rate, might become dominant at geological strain rates.

APPARATUS AND TECHNIQUE

The specimens were deformed in a high-pressure, high-temperature apparatus built and described by Paterson (1970). This apparatus has three major features indispensable for rheological investigations at low stresses and high temperatures: gas-confining medium, internal heating and internal load cell. Load fluctuations of less than 5 kg (corresponding to ~6 bars) can be detected. Temperatures can be easily kept at least within ±5°C of the nominal temperature over the entire length of the specimen.

Cores of 10 mm diameter and 20 mm length (unless stated otherwise in Table I) were drilled perpendicular to bedding. The specimens were jacketed in thin-walled copper jackets (0.25 mm wall thickness). All tests were compressional using a standard confining pressure of 3 kbar and temperatures between 600 and 900°C. Most of the experiments were performed at constant motor speed (corresponding to constant strain rate once steady-state flow is achieved) and at the end of many of those runs stress-relaxation tests were performed (Table I).

The stress—strain curves were derived by making the usual corrections for apparatus distortion, copper strength and cross-section increase with increasing strain. Strain rates listed were computed near 10% strain.

After straining the specimen the temperature was immediately lowered in order to avoid annealing of the structure and grain growth.

EXPERIMENTAL RESULTS

Constant strain-rate tests

The stress—strain curves exhibit no appreciable variation in stress after a few percent strain under all test conditions. The flow stress used for establishing strain rate vs. stress relationships was taken at 10% strain. Figure 1

Notes belonging to Table I

All tests were performed at constant strain rate and on samples of 10 mm diameter and 20 mm length unless stated otherwise:

* Specimen of 7 × 14 mm.

** Creep test.

*** Change of strain rate within one test.

The numbers assigning the tests to different flow regimes stand for:

1: $\dot{\epsilon} \propto \exp(C\sigma)$

2: $\dot{\epsilon} \propto \sigma^n$/high n-values

3: $\dot{\epsilon} \propto \sigma^n$/low n-values

R: Stress-relaxation test at the end of the run.

TABLE I

List of experiments

Run number		Temperature (°C)	Strain rate at 10% strain (sec^{-1})	Differential stress at 10% strain (bar)	Flow regime
2630	R	600	$6.6 \cdot 10^{-3}$	2419	1
2623		600	$3.4 \cdot 10^{-3}$	2467	1
2617		600	$9.9 \cdot 10^{-4}$	2189	1
2621		600	$9.8 \cdot 10^{-4}$	2137	1
2560*	R	600	$9.5 \cdot 10^{-4}$	2043	1
2619		600	$3.1 \cdot 10^{-4}$	1886	1
2644	R	600	$1.5 \cdot 10^{-4}$	1870	2
2604	R	600	$8.6 \cdot 10^{-5}$	1663	2
2624		600	$3.5 \cdot 10^{-5}$	1310	2
2660**	R	600	$2.9 \cdot 10^{-5}$	1315	2
2550*	R	600	$1.0 \cdot 10^{-5}$	1070	2
2628		600	$1.0 \cdot 10^{-5}$	990	3
2622		600	$5.4 \cdot 10^{-6}$	640	3
2651		600	$3.8 \cdot 10^{-6}$	680 (at 7.4%)	3
2654**		600	$7.3 \cdot 10^{-7}$	368 (at 6.5%)	3
2599	R	700	$6.3 \cdot 10^{-3}$	1693	2
2632		700	$2.0 \cdot 10^{-3}$	1232	2
2565*	R	700	$1.0 \cdot 10^{-3}$	1146	2
2551*	R	700	$9.9 \cdot 10^{-4}$	1137	2
2636		700	$3.5 \cdot 10^{-4}$	930	2
2547*		700	$1.5 \cdot 10^{-4}$	676	2
2613	R	700	$1.1 \cdot 10^{-4}$	561	3
2654**		700	$2.6 \cdot 10^{-5}$	368	3
2641		700	$2.1 \cdot 10^{-5}$	349	3
2655**		700	$1.8 \cdot 10^{-5}$	271	3
2606		700	$1.4 \cdot 10^{-5}$	234	3
2631		700	$1.0 \cdot 10^{-5}$	205	3
2610		700	$5.2 \cdot 10^{-6}$	147	3
2592	R	800	$6.4 \cdot 10^{-3}$	858	2
2642		800	$6.3 \cdot 10^{-3}$	770	2
2648		800	$2.0 \cdot 10^{-3}$	645	2
2559*	R	800	$1.0 \cdot 10^{-3}$	622	2
2561	R	800	$7.6 \cdot 10^{-4}$	622	2
2662	R	800	$6.1 \cdot 10^{-4}$	448	3
2646	R	800	$3.5 \cdot 10^{-4}$	397	3
2549*		800	$1.4 \cdot 10^{-4}$	184	3
2557	R	800	$1.3 \cdot 10^{-4}$	305	3
2608	R	800	$8.5 \cdot 10^{-5}$	242	3
2668		800	$7.1 \cdot 10^{-5}$	115	3
2554*		800	$9.4 \cdot 10^{-6}$	88	3
2591		800	$9.0 \cdot 10^{-6}$	87	3
2595		900	$7.1 \cdot 10^{-3}$	371	2
2671***		900	$7.9 \cdot 10^{-4}$	196 (13%)	3
2569		900	$6.7 \cdot 10^{-4}$	277	3
2671		900	$3.8 \cdot 10^{-4}$	134	3

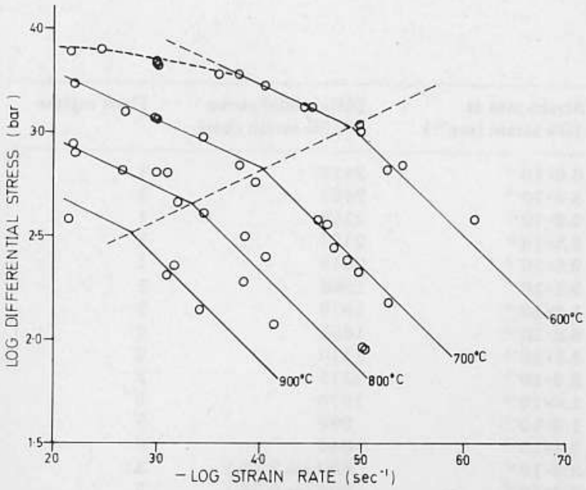

Fig. 1. Log $\dot{\varepsilon}$ vs. log σ diagram. Data points correspond to those listed in Table I. The lines of best fit correspond to the values listed in Table II.

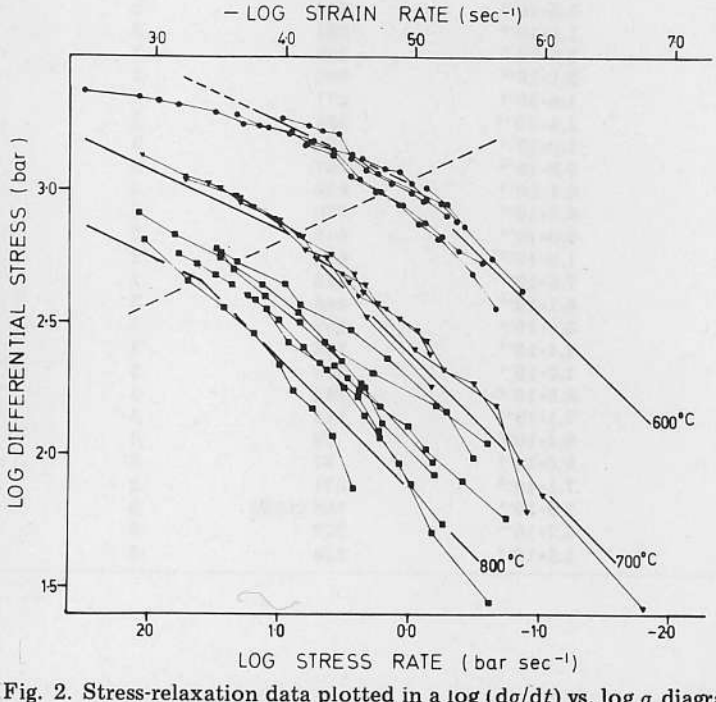

Fig. 2. Stress-relaxation data plotted in a log $(d\sigma/dt)$ vs. log σ diagram. Points belonging to one relaxation test are interconnected by lines. Circles, triangles and squares stand for test temperatures of 600, 700 and 800°C, respectively. The stress rates on the top scale were calculated using eq. 2. For comparison the lines of best fit for the data points in Fig. 1 are superimposed.

shows all the results listed in Table I in a strain rate/stress diagram with logarithmic axes. Tests at a given temperature lie along a straight line in this diagram if a constitutive equation of the following form (Stocker and Ashby, 1973) holds:

$$\dot{\epsilon} = A \exp\left(\frac{-E}{RT}\right)\sigma^n \tag{1}$$

A and n are constants, E is the apparent activation energy for creep, R the gas constant and T the temperature in °K.

It is obvious from first inspection of Fig. 1 that no single relationship of the form of eq. 1 is valid for all the laboratory conditions covered. It was found that all the data below 1900 bars can be satisfactorily described by two sets of parameters in eq. 1. Individual tests in the transition region were assigned to one of the two sets such as to optimize a least-square fit to the linearized form of eq. 1 (Table II). No statement can be made about the width of the transition zone, nor can the existence of minor variations in n as a function of stress be excluded within each of the data groups, given the scatter in the data available. Thus three equations, possibly implying three distinct deformation mechanisms, fit the entire range of σ, $\dot{\epsilon}$ and T covered:

(1) An exponential relationship of the form $\epsilon \propto \exp(C\sigma)$ is suggested for stresses above ~1900 bars at 600°C. Thus the few data in this range fall approximately on a straight line in a $\log_{10} \dot{\epsilon}$ vs. σ plot. The slope $C(\ln 10)$ lies around 2.0—2.2 kbar^{-1}.

(2) A region of power-law creep with high n-values around 4.5 and an apparent activation energy for creep of ~68 kcal./mole.

(3) A region of power-law creep with low n-values around 2.0 and a reduced activation energy of ~50 kcal./mole.

TABLE II

Values for log A, H and n obtained from a least-square fit to the linearized form of eq. 1 (first standard deviation)

	log A (sec^{-1} bar^{-n})	H(kcal./mole)	n
High-stress regime	−0.88 ± 1.79	68.4 ± 9.3	4.35 ± 1.03
Low-stress regime	1.55 ± 1.02	50.4 ± 5.9	2.05 ± 0.43

Not much can be said about the transition of exponential into power-law creep in σ—$\dot{\epsilon}$—T-space since this transition was observed at 600°C only. An exponential flow law well describes the behaviour of Solenhofen limestone at temperatures below 600°C with $C(\ln 10)$~2.7 kb^{-1}, (Rutter, 1974). A similar transition into power-law creep was shown by Heard and Raleigh (1972) to occur in Yule marble, in this case at lower stresses around 1100—1400 bars at 500°C.

The second change from high n-values to low n-values takes place at a transition stress which rises from 300 bars at 900°C to 1050 bars at 600°C. This suggests that at upper-crustal temperatures of less than 600°C the entire range of geologically realistic flow stresses may lie below this transition in the case of fine-grained calcite rocks.

Stress-relaxation tests

Stress-relaxation tests were performed at the end of many of the constant-strain-rate tests (Table I) by simply stopping the crosshead movement and monitoring the stress drop in the specimen as a function of time. This stress drop is due to creep in the specimen as elastic strains in specimen and apparatus are converted into permanent strain in the specimen. Strain rate in the specimen is related to the "stress rate" ($d\sigma/dt$) by:

$$\dot{\epsilon}_s = (L_a K_a + K_s)\,\frac{d\sigma}{dt} \tag{2}$$

where K_a and K_s are the elastic compliances of apparatus and specimen, respectively; L_a converts apparatus displacement into permanent specimen strain.

Figure 2 shows the results in the form of a log stress/log stress rate diagram. If apparatus distortion is constant and under the assumption that the specimen readjusts itself continuously to strain rates described by eq. 1 as the stress drops (i.e. remains in steady state), the right-hand sides of eqs. 1 and 2 are equal. Thus the plots in Figs. 1 and 2 should contain identical information and stress rates in Fig. 2 are converted into strain rates using eq. 2.

To test the assumption just made and thereby the validity of a stress-relaxation test for investigating the form of constitutive equations of creep, the best fits obtained from the constant-strain-rate data (Fig. 1) have been superimposed on the relaxation data in Fig. 2.

Although there is considerable scatter at low stresses (800° runs) the agreement is surprisingly good. This makes the stress-relaxation test a powerful tool to investigate a wide range of stresses and even to detect changes in deformation mechanisms (reflected in a change in slope n on a log σ/log($d\sigma/dt$) plot) in one single test.

DISCUSSION

The most significant observation in view of extrapolations to geological conditions is clearly the transition from high n-values ($n \sim 4.5$) to low n-values ($n \sim 2$) in a power-law relationship (eq. 1). At differential stresses of the order of magnitude expected in most geological situations (less than 1 kb) the deformation mechanism leading to low n-values ($n \sim 2$) is expected to dominate in fine-grained calcite rocks. It is interesting to note that such a transition into low n-values has not been reported on coarser-grained Yule marble (average grain size 400 μm) even down to stresses as low as 150 bars at 800°C (Heard and Raleigh, 1972). This suggests that the transition into the low n-values is grain-size dependent. Another fact emerging from a comparison with Yule marble is that Solenhofen limestone is relatively stronger than Yule marble at moderate temperatures and/or high strain rates but becomes relatively weaker at high temperatures and/or low strain rates.

It is the task of further work currently being undertaken in this laboratory (1) to establish the grain-size dependence of this transition into low-n creep and (2) to reveal the exact nature of the deformation mechanisms bringing about the changes in rheology. Evidence for substantial grain-boundary sliding in the $n \sim 2$ region is already available from the observation that the total strain in the specimen is only partially recorded by the flattening of individual grains in this flow regime (for example less than 1/3 of a total strain of 35% in test 2632 at 900°C is brought about by grain flattening alone). The lower activation energy for creep in the $n \sim 2$ region is interesting in this context because grain-boundary diffusion (a possible process of grain-boundary accomodation) generally exhibits lower values of activation energy than bulk diffusion (Stocker and Ashby, 1973).

Grain-size-dependent creep is to be expected in deformation regimes such as diffusional flow (Coble- and Nabarro-Herring creep). These models however predict a linear stress—strain rate relationship. A phenomenon referred to as superplastic flow in the metallurgical literature however has striking similarities with what is reported here. The mechanisms leading to superplastic behaviour are not fully known (Ashby and Verrall, 1973, suggest diffusion-accomodated grain-boundary sliding) but most metallurgical authors report the following characteristics of superplastic flow (review by Davies et al., 1970):

(1) Low n-values ($1<n<3$) in a constitutive equation in the form of eq. 1.

(2) Stable grain size of $<10\ \mu m$*, the grains remaining equiaxed up to high strains.

(3) Low dislocation density and destruction of preferred orientation.

The low n-values described above suggest that superplasticity occurs at low stresses in Solenhofen limestone supported by the observation of a persistence of equiaxed grains and the absence of substantial grain growth. Although based on field evidence alone, Boullier and Gueguen (1975) regard superplasticity as an important deformation mechanism in some fine-grained mylonites. It is interesting that an extrapolation based on the constitutive equations derived here (Table II) brings the stress down to reasonable values at strain rates inferred from field data along the Glarus overthrust, a thrust involving flow of an ultra-fine-grained calcite mylonite layer (Schmid, 1975).

ACKNOWLEDGEMENTS

I am grateful to M.S. Paterson for providing me with an excellent deformation apparatus. Discussions with J.N. Boland, M.S. Paterson and E.H. Rutter

* This boundary of 10 μm cited in the metallurgical literature might not apply under geological strain rates.

were most rewarding. J.N. Boland and T.J. Fitch helped with computing problems in data processing. G.T. Milburn and P. Willis provided technical assistance.

REFERENCES

Ashby, M.F. and Verrall, R.A., 1973. Diffusion-accommodated flow and superplasticity. Acta Metall., 21: 149—163.

Boullier, A.M. and Gueguen, Y., 1975. Origin of some mylonites by superplastic flow. Contrib. Mineral. Petrol., 50: 93—104.

Davies, G.J., Edington, J.W., Cutler, C.P. and Padmanabhan, K.A., 1970. Superplasticity: A Review. J. Mater. Sci., 5: 1091—1102.

Heard, H.C., 1963. Effects of large changes in strain rate in the experimental deformation of Yule marble. J. Geol., 71: 162—195.

Heard, H.C. and Raleigh, C.B., 1972. Steady-state flow in marble at 500—800°C. Geol. Soc. Am. Bull., 83: 935—956.

Paterson, M.S., 1970. A high-pressure high-temperature apparatus for rock deformation. Int. J. Rock Mech. Min. Sci., 7: 517—526.

Paterson, M.S., 1975. Some current aspects of experimental rock deformation. Paper presented at meeting on "Natural strain and geological structure", Royal Society London, March 1975 (to be published).

Rutter, E.H., 1974. The influence of temperature, strain rate and interstitial water in the experimental deformation of calcite rocks. Tectonophysics, 22: 311—334.

Rutter, E.H., 1975. The kinetics of rock deformation by pressure solution. Paper presented at meeting on "Natural strain and geological structure", Royal Society London, March 1975 (to be published).

Schmid, S.M., 1975. The Glarus overthrust: Field evidence and mechanical model. Eclogae Geol. Helv., 68: 251—284.

Stocker, R.L. and Ashby, M.F., 1973. On the rheology of the upper mantle. Rev. Geophys. Space Phys., 11: 391—426.